Addressing temperature effects on metal chemodynamics studies using stripping electroanalytical techniques. Part 1: Lability of small complexes

Elise Rotureau, Yves Waldvogel, Romain M. Présent, Jose Paulo Pinheiro

Addressing temperature effects on metal chemodynamics studies using stripping electroanalytical techniques. Part 1: Lability of small complexes

Elise Rotureau[1,2*], Yves Waldvogel[1,2], Romain M. Présent[1,2], Jose Paulo Pinheiro[1,2]

[1] CNRS, LIEC (Laboratoire Interdisciplinaire des Environnements Continentaux), UMR7360, Vandoeuvre-lès-Nancy F-54501, France.

[2] Université de Lorraine, LIEC, UMR7360, Vandoeuvre-lès-Nancy, F-54501, France.

* Corresponding author: elise.rotureau@univ-lorraine.fr

Abstract

Temperature effects on metal speciation dynamics were studied using Stripping Chronopotentiometry at Scanned deposition Potential (SSCP). The temporal and spatial scales of this study are respectively O(10^{-1}s) and O(10^{-5}M), characteristics of the thin mercury film rotating disk, used as working electrode. The lability degree and the association rate constant were evaluated in the temperature interval of 15 to 40°C for a significantly non-labile system, cadmium binding by nitrilotriacetic acid, and a quasi-labile system, lead binding by iminodiacetic acid. The results for both systems reveal that the lability of the metal complex significantly increases with temperature. This lability gain results from the thermal augmentation of the association rate constant and the broadening of the diffusion layer thickness.

An evaluation of the metal calibration methodology for SSCP at different temperatures was conducted. It was found that although the variation of diffusion layer thickness can be correctly predicted, changes in standard reduction potential of the metals cannot, thus a calibration must be performed for each temperature studied.

This work constitutes a first step toward the comprehension of the effect of temperature on metal chemodynamics.

Keywords: dynamic metal speciation, lability, scanning stripping chronopotentiometry, thin mercury film electrode, temperature effects, nitrilotriacetic acid (NTA), iminodiacetic acid (IDA)

Introduction

Temperature is a key parameter in electrochemical experiments since it directly affects both the thermodynamics and kinetics of the chemical reactions and the transport of the species from the bulk to the electrode surface.

Thermoelectrochemistry is the branch of electrochemistry that focuses on the variation of the temperature as an independent variable. The increase of temperature is obtained by various means, either directly (heating the working electrode) or indirectly (using microwaves to heat the solution) and the experiments can be performed isothermally or non-isothermally.[1] One interesting analytical aspect is that due to the increased mass transport at high-temperatures higher current signals are obtained, hence lower detection limits.[2]

Unfortunately there are very few metal chemodynamics or even metal speciation studies at different temperatures although they are certainly significant as demonstrated recently by Hassler *et al* [3] in the study of iron speciation in seawater at 4°C.

For metal speciation studies the common practice is to work at constant temperature, usually by thermostating the working solution, nevertheless there are some situations where this is not possible, for example, during on-site studies in environmental waters ranging from almost freezing conditions in cold climates to warm waters in tropical regions.

In other situations the objective is to examine the effect of temperature, like in the case of the studies of metal interactions with thermoresponsive polymer nanoparticles in which we are especially interested. In recent years there has been an increasing interest in these particles due to their ability to change their properties, such as dimension, structure, interactions, or aggregation state, in response to external stimuli (temperature, pH, pressure, ionic strength, etc.). [4,5]

Chemodynamic modeling requires both the knowledge of thermodynamic equilibrium parameters and the kinetics of the interconversion of metal complex species. Stripping electroanalytical techniques, like Stripping Chronopotentiometry at Scanned deposition

Potential (SSCP) are able to provide thermodynamic and kinetic information at the very low concentration levels of metals concentrations in environmental samples. [6,7] Effectively the signal of the stripping electroanalytical techniques is determined by the diffusion and/or kinetic fluxes of the various metal species in solution, both depending on the time-scale of the technique and on the intrinsic characteristics of the complexing species.

The main scientific question of this study concerns the effect of temperature on metal complex lability, especially due to the different influence of temperature on some key parameters. For example the thickness of the reaction layer is affected by the ratio of the diffusion coefficient and the association rate constant of the metal, which both increase with temperature

Additionally there is a methodological question regarding the possibility of performing the calibration at only one temperature followed by complexation studies at different temperatures. This will depend on our ability to predict both the variations of diffusion coefficients (D_M) and standard potential of reduction and amalgamation of the metal species $E°(M^{n+}/M(Hg))$ at different temperatures.

Theory

The theoretical basis for stripping chronopotentiometry (SCP), and its use in SSCP are well established.[6,7] In this work we are using a thin mercury film electrode (TMFE) assembled in a rotating disk electrode that has been thoroughly characterized for SSCP experiments.[8] The principles and key equations relevant for the present work, including the temperature effects, are briefly recalled here.

Metal ions in absence of ligand: SCP limiting current

In stripping chronopotentiometry the number of moles reduced during the deposition step equals the number of moles reoxidized during the stripping step. The limiting transition time (τ_M^* in s) given by:

$$\tau_{\mathrm{M}}^{*} = I_d^{*} t_d / I_s \quad (1)$$

where t_d (s) is the deposition time, I_s (A) the stripping current and I_d^{*} (A) is the limiting value of the deposition current.

I_d^{*} which by definition is obtained for deposition potentials (E_d) that are sufficiently negative, so that the concentration of metal ions at the electrode surface approaches zero ($c_{\mathrm{M}}^{0} \rightarrow 0$), is given by:

$$I_{\mathrm{d}}^{*} = \left(nFAD_{\mathrm{M}} c_{\mathrm{M}}^{*}\right) / \delta_{\mathrm{M}} \quad (2)$$

where c_{M}^{*} (mol.m^{-3}) is the metal concentration in the bulk solution, A is the electrode surface area (m²), D_{M} is the diffusion coefficient of the metal ion (m².s^{-1}), n is the number of electrons involved in the reduction, F (C.mol^{-1}) is the Faraday constant and δ_{M} (m) is the diffusion layer thickness. For the rotating disk electrode (RDE) the thickness of the diffusion layer is expressed by [9]:

$$\delta_{\mathrm{M}} = 1.61 D_{\mathrm{M}}^{1/3} \omega^{-1/2} \upsilon^{1/6} \quad (3)$$

where ω (s^{-1}) is the angular speed rotation for the RDE ($\omega = 2\pi\nu_{\mathrm{rot}}$, where ν_{rot} is the speed of rotation) and υ is the kinematic viscosity of the solution (m².s^{-1}).

The variation of the diffusion coefficient of the metal with temperature follows Stokes-Einstein equation given by [10]:

$$D_{\mathrm{M}} = k_{\mathrm{B}} T / 6\pi\eta r_{\mathrm{h}} \quad (4)$$

where k_{B} (J.K^{-1}) is the Boltzmann constant, r_{h} (m) is the hydrodynamic radius of the diffusion species, T (K) is the temperature and η (Pa.s) is the absolute viscosity of the solution, given in table 1. The variation of viscosity (absolute and kinematic) with temperature was obtained from NIST recommended values.[11]

The thermal expansion of mercury in the range of temperatures used (288 to 318 K) is found negligible since it follows the respective variation in density which is –0.54%.[12]

Similarly the bulk concentration of metal will be affected by the thermal expansion of water, for which the water density variation is 0.63% (from 288 to 318 K).[13] Both these volume variations are well below the experimental error of these experiments, so that both the mercury electrode area and volume and the metal concentration are assumed to remain constant within the range of temperatures tested.

From eqs 2, 3 and 4 it can be seen that the limiting current depends directly on the temperature through the diffusion coefficient and indirectly through the diffusion layer δ_M dependence on the kinematic viscosity

Metal ions in absence of ligand: SSCP half-wave potential

The SSCP general equation that describes the relationship between τ and E_d is [7]:

$$\tau = \left(I_d^* \tau_d / I_s\right)\left[1 - \exp\left(-t_d/\tau_d\right)\right] \quad (5)$$

where τ (s) is the transition time, τ_d (s) is the characteristic time constant for the deposition process, which for a TMFE is defined by:

$$\tau_d = V\delta_M / \left(AD_M\theta\right) \quad (6)$$

For a TMFE, the volume of the electrode (V in m^3) can be estimated from the charge for reoxidation of the film (Q_{Hg} in C) using Faraday's law and the mercury density:

$$V = M_{w,Hg} Q_{Hg} / 2Fd_{Hg} \quad (7)$$

The parameter θ is the ratio of the surface concentrations ($\theta = c_M^0 / c_{M^0}^0$) for the reversible electron transfer reaction, $M^{n+} + ne^- \leftrightarrow M^0$. At a given deposition potential E_d, this parameter is calculated using the following Nernst type equation:

$$\theta = \exp(nF(E_d - E^{0'})/RT) \quad (8)$$

where, R ($J.mol^{-1}.K^{-1}$) the gas constant and $E^{0'}$ (V) is a parameter related to the standard potential of reduction for the amalgamation reaction relative to the reference electrode used and the ionic strength of the solution. In SSCP the usual potential parameter is the half-wave

potential ($E_{1/2}$) which is a function of $E^0_{Mn+/M(Hg)}$, temperature, ionic strength, diffusion coefficients of the metal amalgamated and in solution, potential of the reference electrode used and the volume of the electrode, *V*. The standard potential of amalgam electrodes in aqueous solutions, their temperature coefficients and the activity coefficients of metals in mercury have been reviewed by Mussini *et al.*[14]

The general scheme of a metal amalgam electrode reaction is:

$$M^{z+} + Hg + ze^- = \{M - Hg\} \quad (9)$$

and for a TMFE, the simplified version of the equation for the metal amalgamation reduction half-wave potential versus the Ag/AgCl reference electrode can be written as:

$$E_{1/2,M} = E^0_{M/\{M-Hg\}} + \frac{RT}{nF} ln \frac{f_M}{f_{\{M-Hg\}}} + \frac{RT}{nF} ln \left(\frac{D_{\{M-Hg\}}}{D_M}\right)^{2/3} - E^0_{Ag/AgCl} \quad (10)$$

where *f* stands for the activity coefficients and *D* for diffusion coefficients in solution (M) and in the amalgam (M-Hg).

The temperature variation of this equation is quite involved since both the activity coefficients, the diffusion coefficients and the standard potentials are temperature dependent, nevertheless Mussini *et al* report a quadratic equation to describe this variation and provide the parameters necessary to perform the computation for several metals.

Chemodynamics: the general equation for metal ions in presence of complexing ligands

Metal chemodynamics theory and investigation by electrochemical techniques have been recently reviewed.[15] Briefly let us consider the case of an electroactive metal ion, M, that forms an electroinactive complex, ML, with a ligand L,

$$\begin{array}{c} \quad k_d \\ M + L \leftrightarrows ML \\ \quad k_a \\ \downarrow\uparrow ne^- \\ M^0 \end{array} \quad (11)$$

where k_a and k_d are the association and dissociation rate constants respectively. The system is dynamic if the rates for the volume reactions are fast on the experimental time scale, *t*:

$$k_d t, \quad k_a^{'} t >> 1 \tag{12}$$

Under conditions of ligand excess we can define:

$$k_a^{'} = k_a c_L \text{ and } K^{'} = k_a^{'} / k_d = K c_L \tag{13}$$

where K (L.mol^{-1}) is the stability constant of ML ($=c_{ML}/c_M c_L$) and c_L ($=\alpha.c_{L,T}$) is the deprotonated concentration of the ligand species involved in the complexation reaction, where $c_{L,T}$ is the total ligand concentration and α is the deprotonation factor.

During reduction of M, the overall flux of free M towards the electrode surface is governed by the coupled diffusion of M and its various complex species, and the kinetics of their interconversion. The concept of lability quantifies the extent to which the complex species dissociate to release free M on the timescale of their diffusion towards the electrode surface.

The steady-state SSCP curve (eq. 5) for dynamic complexes influenced by homogeneous kinetics was deduced on the basis of the Koutecký-Koryta approximation.[16] The parameters I_d^* and τ_d in presence of small ligands, where the complex as the same diffusion coefficient as the free metal, are then given by [17]:

$$I_d^* = nFAc_M^* \left(\frac{\delta_M - \mu}{D_M (1 + K')} + \frac{\mu}{D_M} \right)^{-1} \tag{14}$$

$$\tau_d = \frac{V_{Hg,TMFE}}{A\theta} \left(\frac{\delta_M - \mu}{D_M (1 + K')} + \frac{\mu}{D_M} \right) \tag{15}$$

where μ (m) is the thickness of the reaction layer, representing the zone adjacent to the electrode surface in which ML can no longer maintain equilibrium with M. In its simplest form the reaction layer thickness is defined by [18]:

$$\mu = \left(D_M / k_a^{'} \right)^{1/2} \tag{16}$$

Thus dividing the limiting current equation in presence of complexes (eq. 12) by the limiting current equation in presence of metal alone (eq. 2) yields an equation depending on K' and μ for non-labile complexes and and K' for labile complexes.

The variation in half-wave potential in presence and absence of complexing ligands ($\Delta E_{d,1/2}$) is determined by the stability of the complexes:

$$\Delta E_{d,1/2} = \left(RT/nF\right)\left[-\ln\left(1+K'\right)-\ln\left(\tau^{*}_{M+L}/\tau^{*}_{M}\right)\right] \quad (17)$$

where τ^{*}_{M+L} (s) is the τ^{*} measured in the presence of ligand. The complex stability constant, K, is obtained from eq.17, the mass balance for the metal and the deprotonated concentration of ligand ($\alpha.c_{L,T}$), in all dynamic situations as long as the system remains fully electrochemically reversible.

Lability criteria

The lability degree ξ is defined as the ratio of the limiting current for dynamic complexes (which is the experimentally measured current, I^{*}_{d}), I_{dyn}, and the current for the same conditions assuming that all complexes are labile, I_{lab} (i.e. computed using the experimental parameters of I_{dyn} and imposing in eq. 14 a value of μ of zero.) both corrected for the free metal contribution, I_{free}, as [19]:

$$\xi = \frac{I_{dyn}-I_{free}}{I_{lab}-I_{free}} \quad (18)$$

This lability degree ranges from near 0 for non-labile systems to 1 for fully labile behaviour and will be strongly dependent on temperature, through both the diffusion coefficients and the rate constants. The temperature effects on lability can be studied using SSCP in non-labile systems.

Material and methods

Reagents and solutions

All solutions were prepared with ultrapure water (MilliQ). Pb(II) and Cd(II) solutions were obtained from dilution of a certified standard solution (Fluka). The ionic strength is set with NaNO3 (Fluka, trace select). Diluted HNO_3 or NaOH solutions (Merck suprapure) were used to adjust the pH. The buffers MES (2-(N-morpholino)ethanesulfonic acid from Sigma) and MOPS (3-(N-morpholino)propanesulfonic acid from Sigma) were prepared from the solids. Stock solutions of the ligands NTA (Nitrilotriacetic acid from Sigma-Aldrich, >99%) and IDA (Iminodiacetic acid from Fluka, >98%), were prepared from the solids.

Apparatus

An Ecochemie Autolab type III potentiostat controlled by GPES 4.9 software (Ecochemie, The Netherlands) was used in conjunction with a Metrohm 663VA stand. The auxiliary electrode was a glassy carbon rod and the reference electrode was an Ag/AgCl electrode. The working electrode was a thin mercury film electrode (TMFE) plated onto a rotating glassy carbon (GC) disk of 2 mm diameter (Metrohm). The preparation of TMFE was repeated daily for each set of experiments. GC electrode was conditioned with a polishing and electrochemical pre-treatment according to the reported cleaning procedure.[20] The thin mercury film was plated on the GC electrode ex-situ with a 0.48 mM mercury (II) nitrate in acidic medium (HNO3 0.75mM, pH 1.9) by electrodeposition at -1.3V for 240s and a rotation rate of 1000 rpm. After experiments, the TMFE was cleaned by successive mercury reoxydations in a 80mM thiocyanate ammonium solution buffered with ammonium acetate (pH 3.4).

Experimental protocol

For the temperature control, a disposable polystyrene cell is placed in a double-walled container relied to refrigerated-heating circulator. The temperature of the solution is set from 15 to 45°C with an accuracy of ±0.1°C.

The experimental protocol for calibration measurement at different temperature consists of preparing a solution made up from 18 ml of pure water, 10 µl of 0.1M HNO_3 and the appropriate amount of 1M $NaNO_3$ to fix the ionic strength at 100mM and leaving the solution under nitrogen bubbling during a few minutes to remove oxygen; a nitrogen blanket is maintained between measurements. The metal is then added in the form of $Pb(NO_3)_2$ or $Cd(NO_3)_2$. The SSCP calibrations are performed at pH lower than 4 so as to obtain the metal predominantly in its free form.

For the Cd-NTA and the Pb-IDA analysis, the experiments are performed as follow. After the metal calibration at a fixed temperature, a given quantity of ligand solution is added to the solution, together with 200 µL of 0.1M of buffer solution *i.e.,* MOPS (pH 8) or MES (pH 6.5), respectively. A sufficient quantity of NaOH is then added to fix the pH at 8 for Cd/NTA solution and 6.5 for Pb/IDA solution. SSCP experiments are then performed in the presence of the ligand in solution.

The SCP experimental parameters are as follows: (i) the deposition step is carried out at the specified deposition potential E_d for a time, t_d 45 s for Pb and 90s for Cd, using a rotation rate of 1500 rpm (ii) a stripping current, I_s of 3 µA for Pb and 2 µA for Cd is applied until the potential reaches a value well past the reoxidation transition plateau. A series of SCP measurements over a range of deposition potentials, E_d, yields the full SSCP waves that are essential in the basic kinetic analysis (see theoretical section).

Results and Discussion

Evaluation of the metal calibration methodology

As the temperature variations affect the calibration procedures, these features need to be evaluated carefully before we proceed to study complexation dynamics.

SSCP experiments with metal alone, also called SSCP calibrations, are used to determine three parameters: the effective electrode area (A), the half-wave potential for the metal ($E_{1/2,M}$) and τ_M^*. Within the studies regularly performed using SSCP, there are different methodologies currently employed. When performing titrations with ligand and/or metal concentration variation, at fixed pH, ionic strength and temperature, the calibrations are usually made under the same conditions as those for the titration. In studies with pH variation, the calibrations are done at low pH and the results extrapolated to different pH values.[21] On the other hand for studies at different ionic strengths (constant pH and temperature) it is necessary to perform a calibration per ionic strength.[22]

The first parameter obtained from the calibration is the effective electrode area. From a theoretical point of view the thin film electrode area should be equal to the geometrical area of the electrode; nevertheless these electrodes are not truly a film but rather an ensemble of mercury microdroplets. The effective area is thus determined from equations (2), (3) and (4) providing that the metal concentration is rigorously known.

When the temperature changes it can be seen that the limiting current (eq. 2) will also vary through the temperature dependence of the diffusion coefficient (eq. 4) and the kinematic viscosity dependence of the thickness of the diffusion layer δ_M (eq.3).

In our work the electrode area should remain constant since the thermal expansion of mercury is negligible in this range of temperatures. Figure 1 shows that for both Cd^{2+} and Pb^{2+} ions the computed effective area is constant within the experimental error for the temperature range investigated. This effective area was obtained using eq.2 with the values of the diffusion coefficient (Table 1) and adjusting the thickness of the diffusion layer δ_M for the respective kinematic viscosity at each temperature (Table 1). Thus for purposes of calibration the effective area, the limiting current (*i.e.* the plateau value of the SSCP curve) can be measured at a given temperature and extrapolated to other temperatures of interest, providing that both the kinematic viscosity and the diffusion coefficient are corrected for each temperature.

For the case of interest the influence of temperature in the potential shift variation, $E_{1/2,M}$ is comprised in equation 10. Still the logarithmic nature of the equation and the number of parameters involved imply that the estimated values are affected by a large error. Then again the computation of $E_{1/2,M}$ (eq. 17) needs an accurate determination of the mercury electrode volume, *V*, for which the reoxidation charge measure normally used is insufficiently precise. Thus, for this type of electrode an absolute value of $E^0_{M/M\text{-}Hg}$ is quite difficult to obtain with a good accuracy, consequently it is necessary to calibrate the system for each individual temperature.

Thermodynamic parameters for the Cd(II)-nitrilotriacetate and Pb(II)-iminodiacetate systems

In this section, we seek to evaluate the robustness of the stripping techniques for the investigation of the temperature dependence of the metal stability constant in presence of small ligands. In the first place, the *K* parameter describing metal complexation are investigated in the temperature range of 15 to 40°C. Figure 2 depicts the evolution with temperature of the stability constant (log *K*) of the cadmium complex species in presence of NTA. Values of *K* are calculated according to the equation (17) with $\Delta E_{d,1/2}$ and τ^*_{M+L}/τ^*_M determined from the analysis of the SSCP curves. On the basis of the van't Hoff relationship ($\frac{d\ln K}{dT} = \frac{\Delta H^0}{RT^2}$ with ΔH^0 being the standard enthalpy of reaction), the expected temperature dependence of the stability constant is also reported. These data are obtained by using the stability constant at 20°C (log *K* = 9.83 at 0.1M ionic strength) and the enthalpy of the formation of a 1:1 complex ΔH^0=-3.97 kcal/mol collected from the literature. [23] The results presented in figure 2, demonstrate that SSCP results are in good agreement with the theoretical prediction. For Pb-IDA (not shown here), there is also a good consistency between the experimental log *K* value of 7.8±0.1 at 20°C and the literature value of 7.45 (at 20°C, in 0.1M KNO_3). [24] Nevertheless, we note that since the experimental error is of the same order of magnitude as the expected variation of the log *K* in the range of temperature 15 to 40°C,

SSCP technique is not sufficiently precise to provide a proper evaluation of the temperature dependence of the stability constant.

Dynamic metal complexes: Cd(II)-nitrilotriacetate and Pb(II)-iminodiacetate

Temperature effects on the lability criteria

To tackle the temperature effect on the lability of a metal complex system, we will consider in this study the simple case of the metal binding with a small molecular ligand where $D_{\mathrm{M}} \cong D_{\mathrm{ML}}$. In such situation, the metal complex formation is solely controlled by the chemical kinetics at the complexing sites.

The values of the lability degree ξ were experimentally determined (eq.18) for the Cd binding with NTA and the Pb binding with IDA (figure 3 (a) and (b)). As expected [25], the Cd-NTA system shows a non-labile behaviour considering the experimental degree of lability lower than 0.1 whereas the Pb-IDA complex displays a quasi-labile behaviour with ξ values ranging from 0.6 to 0.8. The figures reveal that, for both Cd and Pb species, the lability degree increases with temperature, particularly significant for Cd complexes with NTA from 15 to 40°C (3 fold increase).

At first this result might appear counterintuitive due to the increase in the stability constant, K with temperature T (see Figure 2) but then again the lability degree is a comparison between currents, i.e. fluxes, thus dependent also on the kinetic and transport properties, namely the thickness of the reaction layer, (μ, experimental value from eq.16) and diffusion layer, (δ_{M} obtained from eq.3 and 4) . From the insets of Figure 3 it is evident that increasing the temperature provokes a significant increase of δ_{M} of *ca.* 1500 nm, while simultaneously μ becomes smaller due to the increase of the association rate constant (eq. 16).

From equation 14 it can be seen that a fully labile system occurs when μ is much smaller than δ_{M}. Therefore the kinetic and transport properties variation with temperature (decreasing μ and increasing δ_{M}) clearly overcomes the effect of the increased stability constant.

Variation of k_a with temperature

The change of the association rate constant, $\log k_a$ (computed using eq. 16 and the experimental value of μ) with the temperature for the Cd-NTA and the Pb-IDA systems is depicted in figure 4. For these type of ligands the exact determination of k_a is difficult due to the influence of the protonated forms of the ligand in the overall metal complexation kinetics as explained by Town *et al*.[26] The different possible reactive pathways imply that in our study the estimated k_a is an effective rate constant weighted by the respective kinetic rate formation of the various complex species. For the outer-sphere complex formation with the Cd^{2+} ions at pH 8, two possible routes can be considered with the formation of $\{CdNTA\}^-$ and $\{CdHNTA\}$ species. Therefore, the experimental values should be compared to the calculated association rate constant accounting for the dehydration rate constant k_w from [27] and the parameter $z_M z_L$ *i.e.* the product of the effective charge of the metal and that of the ligand, equals to -6 or -4. For the same reasons, the theoretical association rate constant are reported for the Pb-IDA system with $z_M z_L$=-4 and -2 corresponding to the formation of the outer-sphere complexes of {PbIDA} and $\{PbHIDA\}^+$, respectively. For the two studied systems, the experimental values of k_a at 298 K are comprised between the two theoretical values, underlying the simultaneous formation of the deprotonated and protonated outer-sphere complexes. To understand the temperature dependence of the association constant kinetics, it is necessary to account for the Eigen-Fuoss mechanism describing the metal complex formation. Considering that the stability constant of the outer-sphere complex K_{os} is mainly dependent of the charge of the reacting species and the ionic strength of the medium, this parameter is not significantly affected by the variation of temperature, at least for that probed in our study. Roughly half of the experimentally observed increase of k_a results from the changes in deprotonation ratio of the ligands (α) with temperature while the rest is likely originated from the variation in the dehydration rate constant k_w. However, to our best knowledge, there are no literature reports on the k_w values as a function of the temperature.

According to our results, we hypothesis that the observed increase in k_w *i.e.* the release of the water molecule from the inner coordination shell is facilitated at higher temperature.

Although the computation of the dissociation rate constant, k_d, is possible using the experimental K' and k_a nevertheless the error associated with the obtained values is too large to allow a meaningful discussion. We can observe that the parameter K increases less with temperature as compared with k_a indicating that k_d should also be increasing with temperature.

Conclusions

The experimental methodology used for the SSCP calibrations was investigated and it was found that for thin mercury film electrodes, it is necessary to calibrate the system for each individual temperature due to the difficulties to predict the shift in the standard potential $E^0_{M/M\text{-}Hg}$ caused by the temperature change.

This study demonstrates that increasing the temperature induces a significant increase of lability of the small metal complex species. This lability variation results from two concomitant processes: (i) the expansion of the thickness of the diffusion layer, due to the increase of diffusion coefficients and decrease of solution viscosity with temperature (ii) the decrease of the reaction layer thickness arising from the augmentation of the association rate constant.

With the small complexes studied here the association rate constant follows a simple Eigen mechanism, while complexation of metal with colloidal ligands generally results from the coupling of the diffusive transport of free-metal ions M and the kinetics of ML complex formation/dissociation within the reactive component of the particle. The kinetic and the mass transport contributions in the association step generally depend on the electrostatic potential, the size, the hydrodynamic and complexation properties of the colloidal dispersions.[28,29]

Therefore studying temperature effects on metal binding with colloidal ligands is an interesting challenge that might reveal quite a different behaviour compared to the small complexes.

References

[1] P. Gründler, A. Kirbs, L. Dunsch, Modern Thermoelectrochemistry, ChemPhysChem. 10 (2009) 1722–1746. doi:10.1002/cphc.200900254.

[2] G.G. Wildgoose, D. Giovanelli, N.S. Lawrence, R.G. Compton, High-Temperature Electrochemistry: A Review, Electroanalysis. 16 (2004) 421–433. doi:10.1002/elan.200302875.

[3] C.S. Hassler, F.-E. Legiret, E.C.V. Butler, Measurement of iron chemical speciation in seawater at 4 °C: The use of competitive ligand exchange–adsorptive cathodic stripping voltammetry, Mar. Chem. 149 (2013) 63–73. doi:10.1016/j.marchem.2012.12.007.

[4] M. Motornov, Y. Roiter, I. Tokarev, S. Minko, Stimuli-responsive nanoparticles, nanogels and capsules for integrated multifunctional intelligent systems, Prog. Polym. Sci. 35 (2010) 174–211. doi:10.1016/j.progpolymsci.2009.10.004.

[5] J.P. Pinheiro, L. Moura, R. Fokkink, J.P.S. Farinha, Preparation and Characterization of Low Dispersity Anionic Multiresponsive Core–Shell Polymer Nanoparticles, Langmuir. 28 (2012) 5802–5809. doi:10.1021/la2045477.

[6] H. van Leeuwen, R. Town, Stripping chronopotentiometry at scanned deposition potential (SSCP). Part 1. Fundamental features, J. Electroanal. Chem. 536 (2002) 129–140. doi:10.1016/S0022-0728(02)01212-3.

[7] R.M. Town, H.P. van Leeuwen, Stripping chronopotentiometry at scanned deposition potential (SSCP): Part 2. Determination of metal ion speciation parameters, J. Electroanal. Chem. 541 (2003) 51–65. doi:10.1016/S0022-0728(02)01314-1.

[8] L.S. Rocha, J.P. Pinheiro, H.M. Carapuça, Evaluation of nanometer thick mercury film electrodes for stripping chronopotentiometry, J. Electroanal. Chem. 610 (2007) 37–45. doi:10.1016/j.jelechem.2007.06.018.

[9] V.G. Levich, Physicochemical hydrodynamics., Prentice-Hall, Englewood Cliffs, N.J., 1962.

[10] A. Einstein, Über die von der molekularkinetischen Theorie der Wärme geforderte Bewegung von in ruhenden Flüssigkeiten suspendierten Teilchen, Ann. Phys. 322 (1905) 549–560. doi:10.1002/andp.19053220806.

[11] J. Kestin, M. Sokolov, W.A. Wakeham, Viscosity of liquid water in the range −8 °C to 150 °C, J. Phys. Chem. Ref. Data. 7 (1978) 941–948. doi:10.1063/1.555581.

[12] G.J.F. Holman, C.A. ten Seldam, A Critical Evaluation of the Thermophysical Properties of Mercury, J. Phys. Chem. Ref. Data. 23 (1994) 807–827. doi:10.1063/1.555952.

[13] W.M. Haynes, CRC Handbook of Chemistry and Physics, 95th Edition, CRC Press, 2014.

[14] T. Mussini, P. Longhi, S. Rondinini, Standard potentials of amalgam electrodes in aqueous solutions, temperature coefficients, and activity coefficients of metals in mercury, Pure Appl. Chem. 57 (1985) 169–179.

[15] A.M. Mota, J.P. Pinheiro, M.L. Simões Gonçalves, Electrochemical Methods for Speciation of Trace Elements in Marine Waters. Dynamic Aspects, J. Phys. Chem. A. 116 (2012) 6433–6442. doi:10.1021/jp2124636.

[16] J. Koutecký, J. Koryta, The general theory of polarographic kinetic currents, Electrochimica Acta. 3 (1961) 318–339. doi:10.1016/0013-4686(61)85008-1.
[17] H.P. van Leeuwen, R.M. Town, Stripping chronopotentiometry at scanned deposition potential (SSCP). Part 4. The kinetic current regime, J. Electroanal. Chem. 561 (2004) 67–74. doi:10.1016/j.jelechem.2003.07.002.
[18] J. Heyrovský, J. Kůta, Principles of Polarography, Academic Press, 1966.
[19] J. Galceran, J. Puy, J. Salvador, J. Cecília, H.P. van Leeuwen, Voltammetric lability of metal complexes at spherical microelectrodes with various radii, J. Electroanal. Chem. 505 (2001) 85–94. doi:10.1016/S0022-0728(01)00475-2.
[20] Monterroso S.C.C., Carapuca H.M., Simao J.E.J., Duarte A.C., Optimisation of mercury film deposition on glassy carbon electrodes: evaluation of the combined effects of pH, thiocyanate ion and deposition potential, Anal. Chim. Acta. 503 (2004) 203–212. doi:10.1016/j.aca.2003.10.034.
[21] E. Rotureau, Analysis of metal speciation dynamics in clay minerals dispersion by Stripping Chronopotentiometry techniques, Colloids Surf. Physicochem. Eng. Asp. (n.d.). doi:10.1016/j.colsurfa.2013.09.006.
[22] D. Goveia, J.P. Pinheiro, V. Milkova, A.H. Rosa, H.P. van Leeuwen, Dynamics and Heterogeneity of Pb(II) Binding by SiO2 Nanoparticles in an Aqueous Dispersion, Langmuir. 27 (2011) 7877–7883. doi:10.1021/la2008182.
[23] G. Anderegg, Critical survey of stability constants of NTA complexes, Pure Appl. Chem. 54 (1982). doi:10.1351/pac198254122693.
[24] G. Anderegg, Komplexone XXXVI. Reaktionsenthalpie und -entropie bei der Bildung der Metallkomplexe der höheren EDTA-Homologen, Helv. Chim. Acta. 47 (1964) 1801–1814. doi:10.1002/hlca.19640470716.
[25] J. Pinheiro, H. van Leeuwen, Scanned stripping chronopotentiometry of metal complexes: lability diagnosis and stability computation, J. Electroanal. Chem. 570 (2004) 69–75. doi:10.1016/j.jelechem.2004.03.016.
[26] H.P. van Leeuwen, R.M. Town, J. Buffle, Impact of ligand protonation on eigen-type metal complexation kinetics in aqueous systems, J. Phys. Chem. A. 111 (2007) 2115–2121. doi:10.1021/jp0673009.
[27] F.M.M. Morel, J.G. Hering, Principles and Applications of Aquatic Chemistry, 1 edition, Wiley-Interscience, New York, 1993.
[28] J.F.L. Duval, J.P.S. Farinha, J.P. Pinheiro, Impact of Electrostatics on the Chemodynamics of Highly Charged Metal–Polymer Nanoparticle Complexes, Langmuir. 29 (2013) 13821–13835. doi:10.1021/la403106m.
[29] H.P. van Leeuwen, J. Buffle, J.F.L. Duval, R.M. Town, Understanding the Extraordinary Ionic Reactivity of Aqueous Nanoparticles, Langmuir. 29 (2013) 10297–10302. doi:10.1021/la401955x.
[30] S. Kariuki, H.D. Dewald, Evaluation of diffusion coefficients of metallic ions in aqueous solutions, Electroanalysis. 8 (1996) 307–313. doi:10.1002/elan.1140080402.
[31] L.S. Rocha, W.G. Botero, N.G. Alves, J.A. Moreira, A.M.R. da Costa, J.P. Pinheiro, Ligand size polydispersity effect on SSCP signal interpretation, Electrochimica Acta. 166 (2015) 395–402. doi:10.1016/j.electacta.2015.03.035.

Table

Temperature (°C)		15	20	25	30	35	40	45
Absolute viscosity (µPa.s)		1138	1002	889	796	718	652	595
Diffusion coefficient (10^{-9} x m²/s)	Cd	5.56	6.37	7.25[(a)]	8.20	9.23	10.8	11.9
	Pb	6.21	7.13	8.10[(b)]	9.17	10.3	12.0	13.3

Table 1: Temperature dependence of the absolute viscosity of water (from Kestin *et al.* [11]) and the diffusion coefficients for Cd^{2+} and Pb^{2+} ions as determined by eq. 4 using the reference values (a) and (b) from [30] and [31], respectively.

Figure captions

Figure 1: Calculated area of the thin film mercury electrode as a function of the temperature. Each area is determined from the plateau value of the SSCP wave for the Pb and Cd solutions and the diffusion coefficient of the metals (see eq. 2). The diffusion coefficients of the metal ions are summarized in the table 1. The inset shows examples of SSCP experimental points and simulated curves (plain lines) obtained for Pb solution ($5x10^{-7}$M) and performed at different temperatures at pH=4 and an ionic strength of 100mM $NaNO_3$.

Figure 2: Estimated log$K$ values corresponding to the formation of the complex Cd with NTA as a function of the temperature. The experimental values are compared to the van't Hoff equation. The total Cd concentration is $2x10^{-6}$M and NTA is set to 10^{-5}M, the ionic strength is fixed to 100 mM $NaNO_3$ and the pH to 8.

Figure 3: Variation of the experimental lability criteria ξ as a function of the temperature for (a) Cd-NTA and (b) Pb-IDA systems. The ionic strength is fixed to 100mM $NaNO_3$ and the pH to 8 for Cd and 6 for the Pb solutions. The inset shows the mean diffusion layer thickness δ_M (open squares) and the reaction layer μ (black squares) for each temperature.

Figure 4: Experimental values of the association rate constant of the complex formation as a function of the temperature for (a) Cd-NTA and (b) Pb-IDA systems. For the Cd-NTA solution, the total Cd concentration is $2x10^{-6}$M and NTA is set to 10^{-5}M, the ionic strength is fixed to 100mM $NaNO_3$, the pH to 8. For the Pb-IDA solution, the total Pb concentration is $5x10^{-7}$M and the IDA concentration is set to 2.6×10^{-3}M, the ionic strength is fixed to 100mM $NaNO_3$, the pH to 6.

Figures

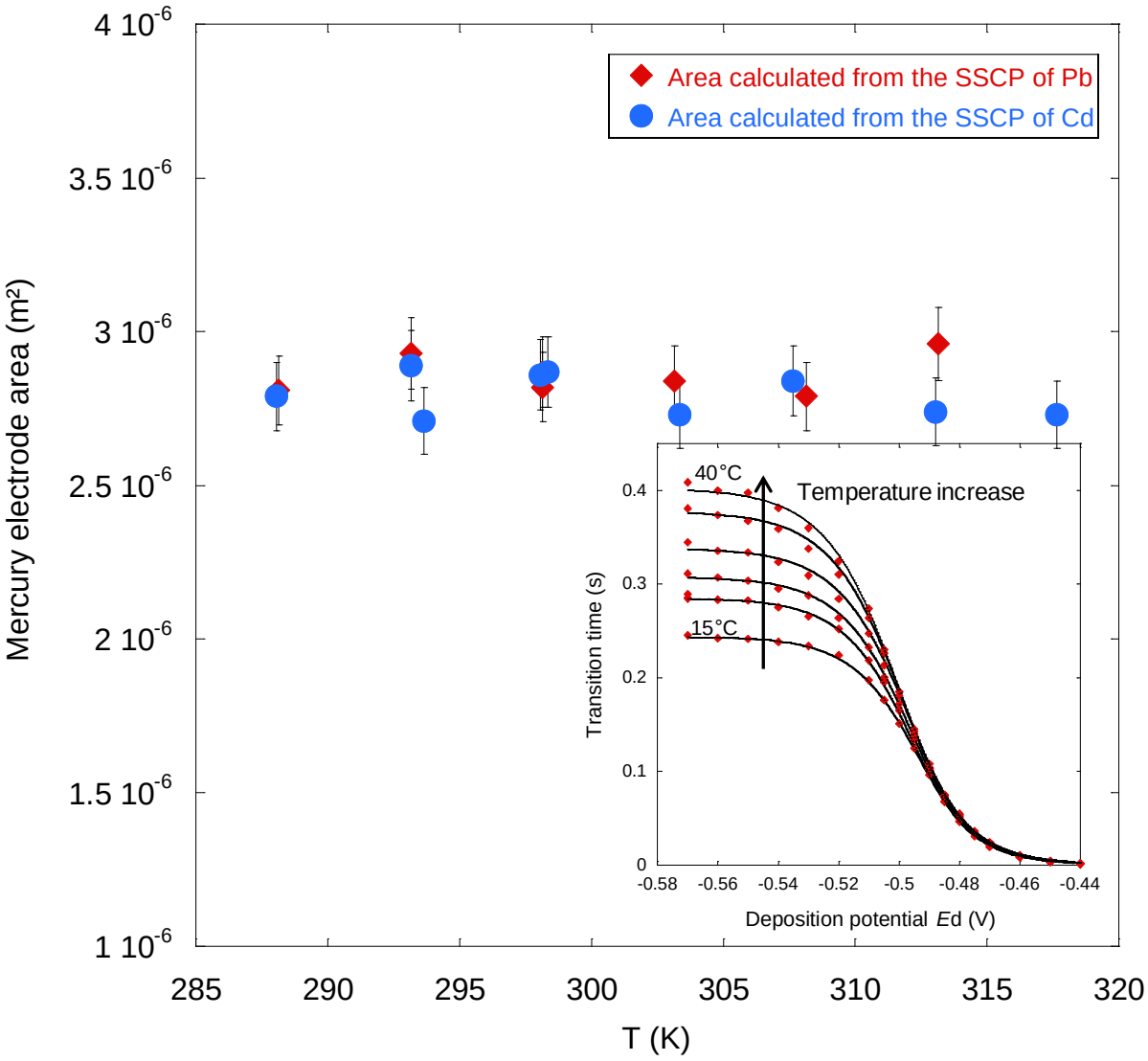

Figure 1

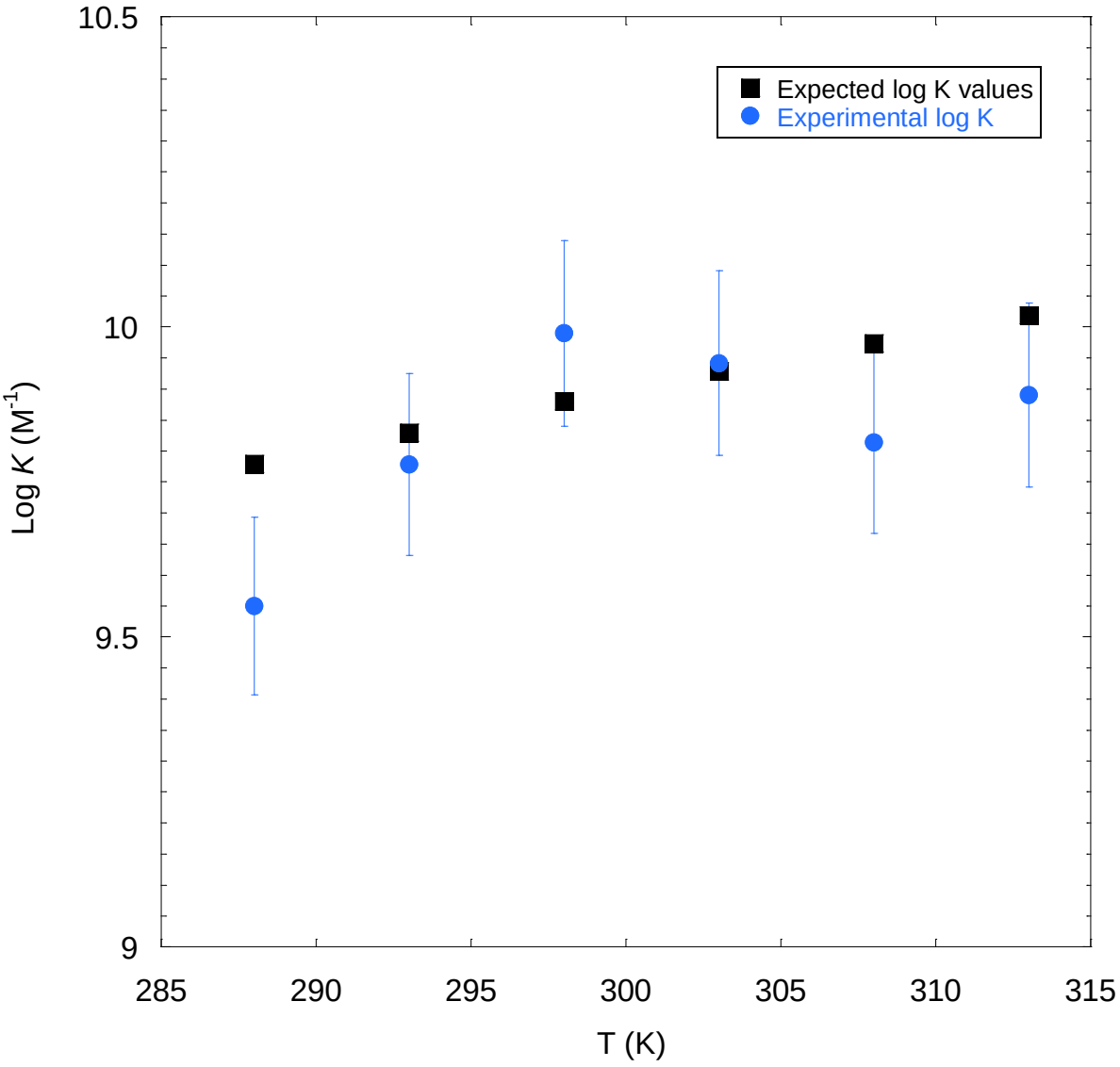

517

518 **Figure 2**

519

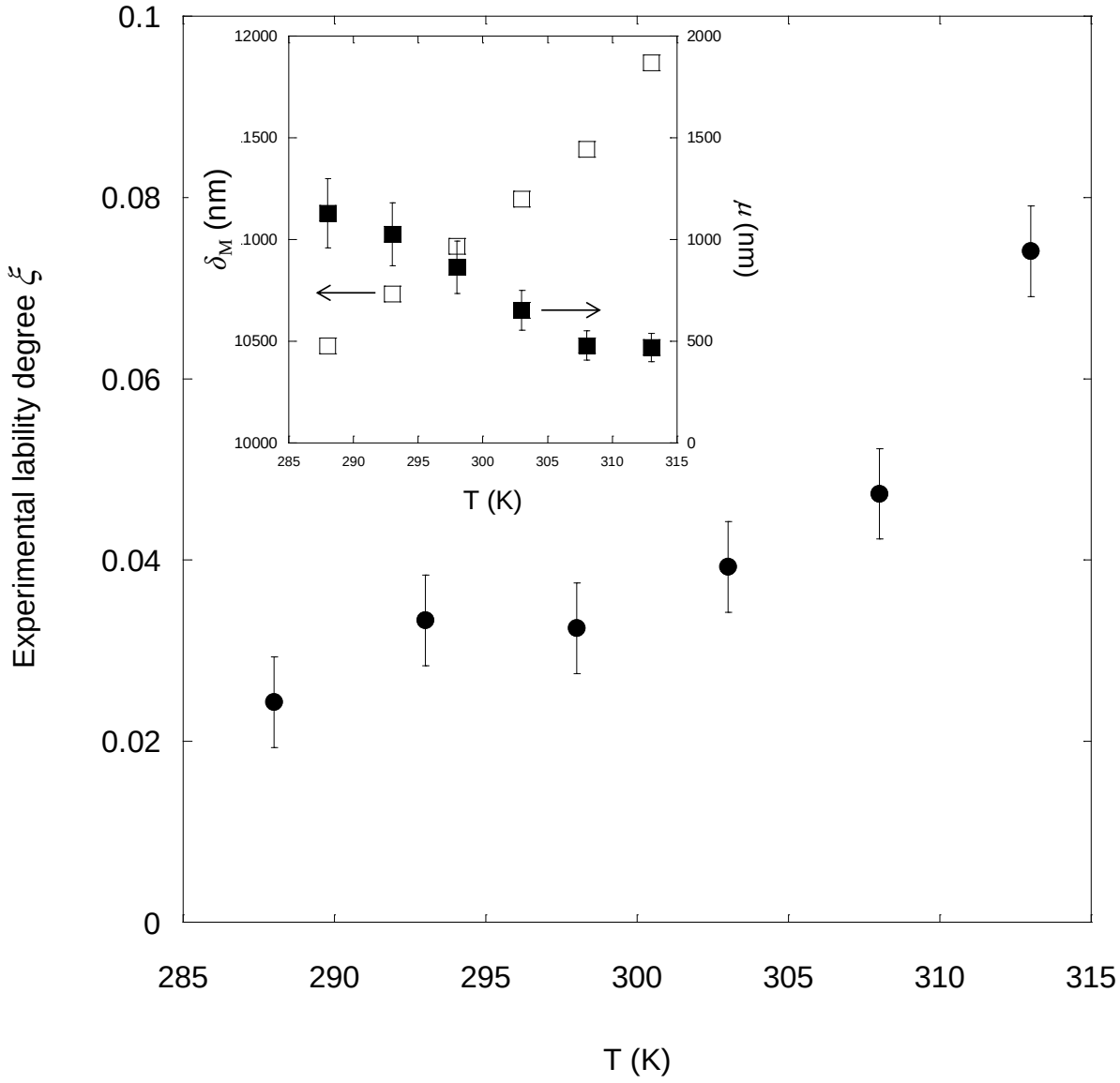

Figure 3 (a)

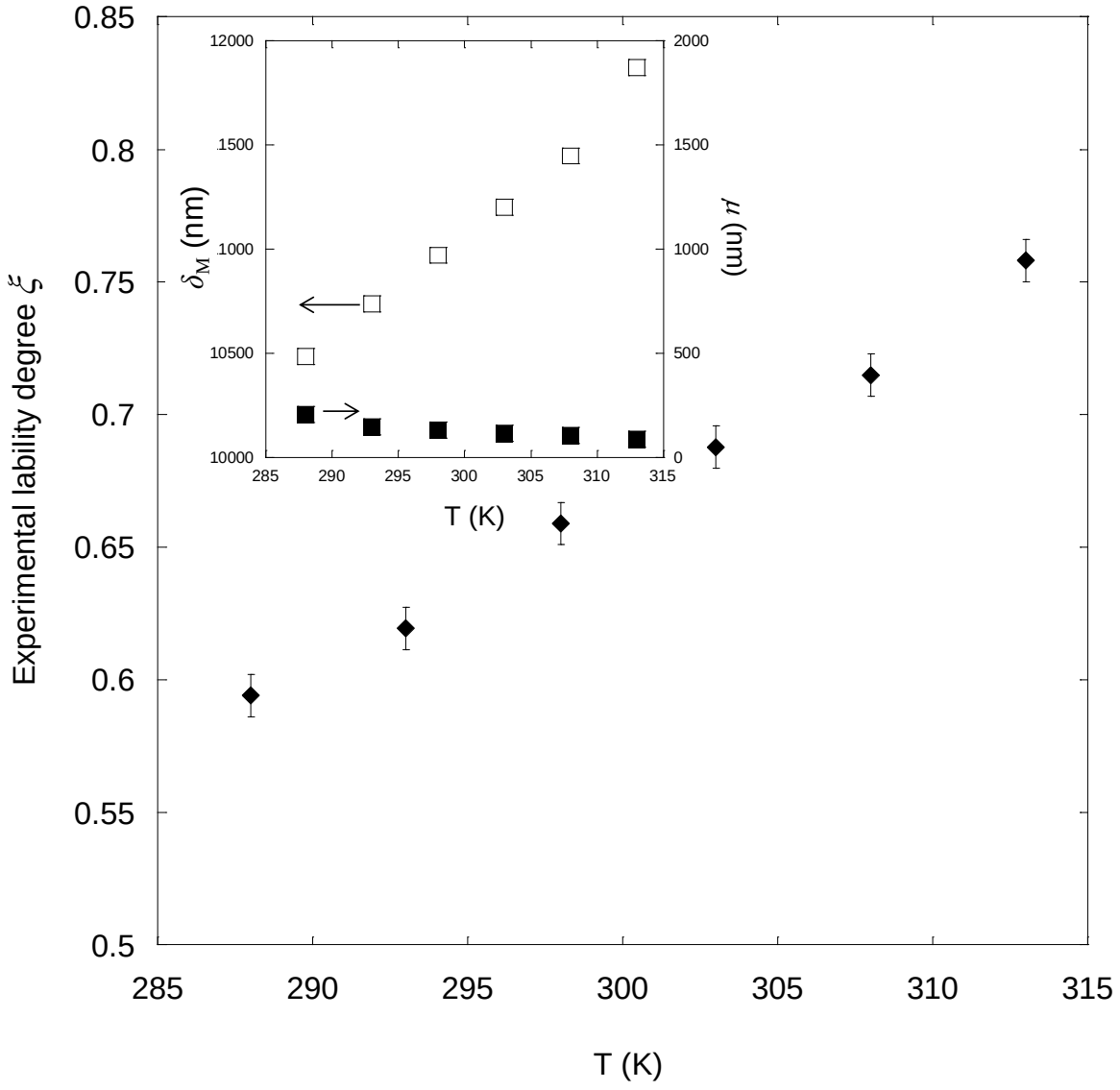

Figure 3 (b)

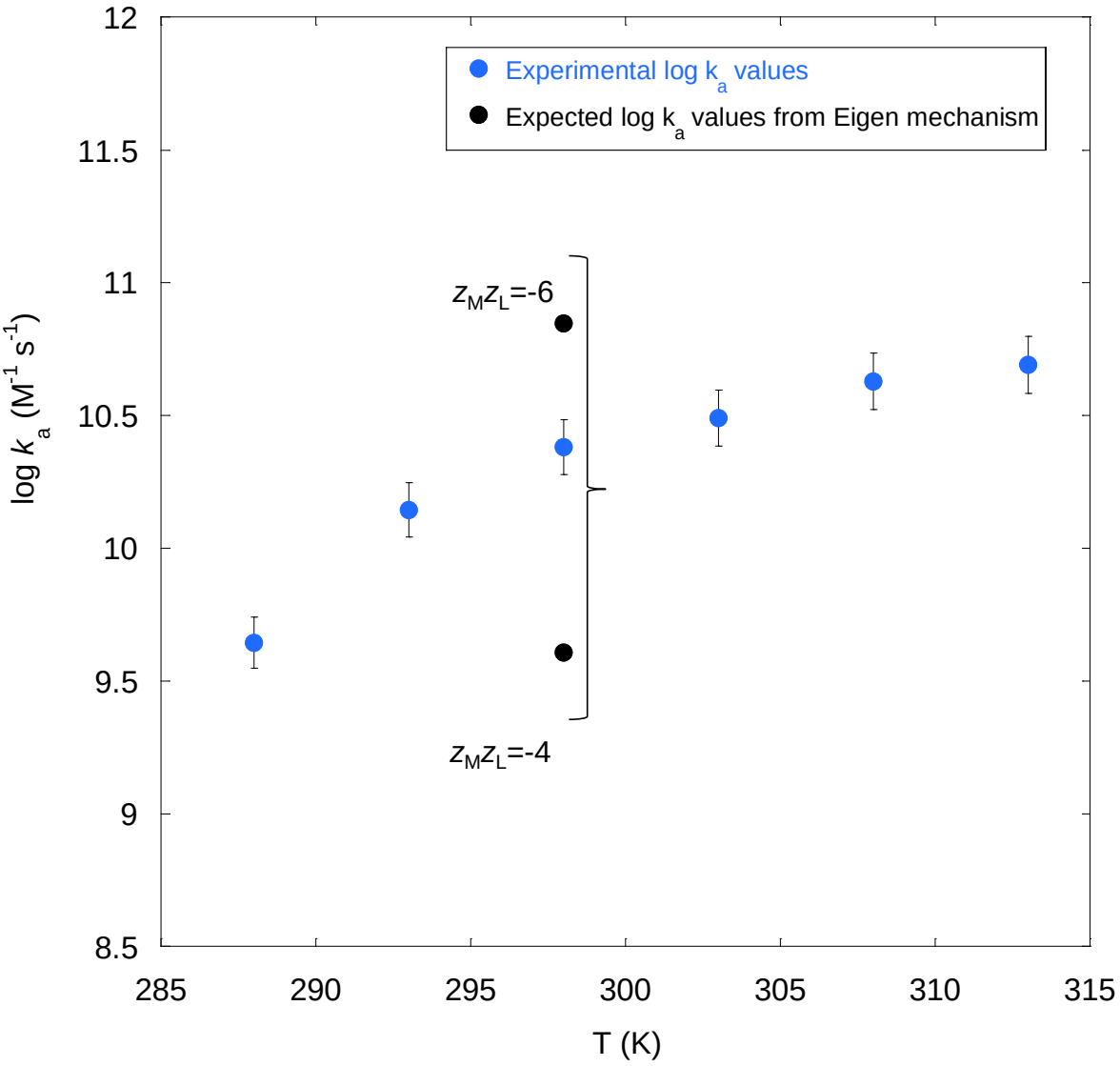

526

527 **Figure 4 (a)**

528

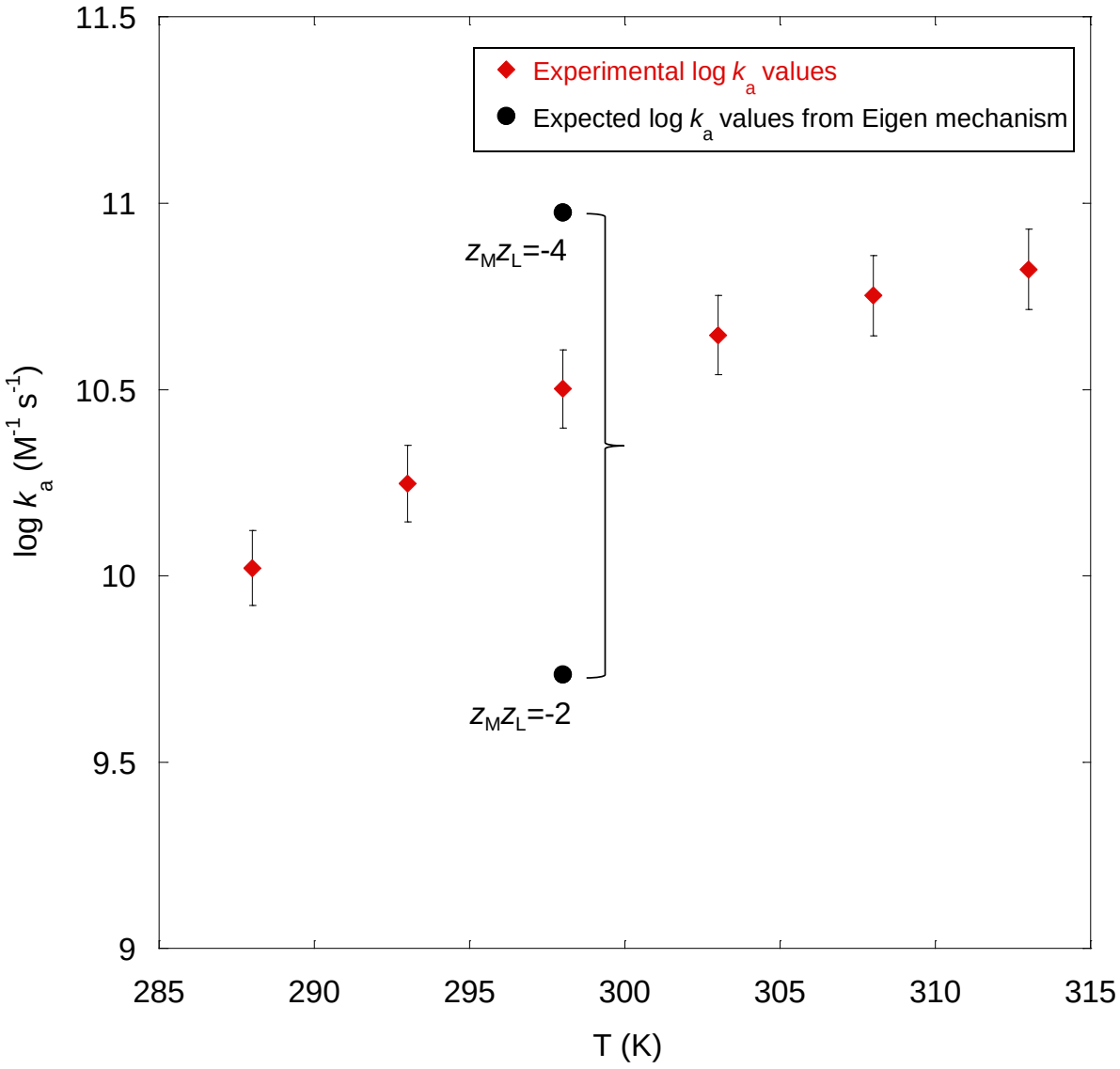
Experimental log k_a values
Expected log k_a values from Eigen mechanism
$z_M z_L$=-4
$z_M z_L$=-2
log k_a (M^{-1} s^{-1})
T (K)
11.5
11
10.5
10
9.5
9
285
290
295
300
305
310
315

Figure 4 (b)